# METALLIC INTERFACES IN HARSH CHEMO-MECHANICAL ENVIRONMENTS

BILGE YILDIZ[1,3], ANNA NIKIFOROVA[1,3] and SIDNEY YIP[2,3*]
[1] Department of Nuclear Science and Engineering, Massachusetts Institute of Technology
Cambridge, MA 02139, USA
[2] Department of Nuclear Science and Engineering and Department of Materials Science and Engineering
Massachusetts Institute of Technology, Cambridge, MA 02139, USA
[3] Center for Advanced Nuclear Energy Systems, MIT
[*]Corresponding author. E-mail : syip@mit.edu

*Received January 29, 2009*

The use of multiscale modeling concepts and simulation techniques to study the destabilization of an ultrathin layer of oxide interface between a metal substrate and the surrounding environment is considered. Of particular interest are chemo-mechanical behavior of this interface in the context of a molecular-level description of stress corrosion cracking. Motivated by our previous molecular dynamics simulations of unit processes in materials strength and toughness, we examine the challenges of dealing with chemical reactivity on an equal footing with mechanical deformation, (a) understanding electron transfer processes using first-principles methods, (b) modeling cation transport and associated charged defect migration kinetics, and (c) simulation of pit nucleation and intergranular deformation to initiate the breakdown of the oxide interlayer. These problems illustrate a level of multi-scale complexity that would be practically impossible to attack by other means; they also point to a perspective framework that could guide future research in the broad computational science community.

**KEYWORDS** : Metallic Interfaces, Multiscale Mode, SCC, Electron Transfer

## 1. INTRODUCTION

The development of advanced energy systems requires materials that can perform at higher temperatures and more aggressive mechanical and chemical environments for longer times. For nuclear applications the additional constraint of coupling to an intense radiation field makes these problems truly formidable. The many challenges faced by materials development for advanced nuclear energy systems have been recently updated [1] in a collection of perspective articles focusing on component applications. These include fuels [2], structural materials [3], ceramics [4], environmental degradation [5], and waste immobilization [6]. In this article, written in a similar spirit, we highlight the challenges and opportunities in the modeling and simulation study of a single materials phenomenon, the breakdown of an interface oxide layer that protects a metal from environmental attack. In contrast to the above articles which emphasize the technological significance of the challenges, we are mostly concerned with fundamental issues in a materials science approach, concentrating on understanding the microstructure and unit processes that lead to constitutive models. Our single-problem focus on the destabilization of the protective oxide layer means we will be correspondingly selective in formulating a multiscale modeling and simulation strategy to carry out the envisaged investigation. In this respect our interest lies in an integrated approach, combining first-principles methods for their electronic-structure rigor with atomistic techniques for dealing with large systems at finite temperatures, all subjected to validation against experiments and taking advantage of key data input along the way from experiments.

Perhaps the most critical issue in the conceptual understanding of corrosion initiation is the role of the interface between the base metal and a fluid environment, the theme of the present discussion. The failure initiation scenario begins with the interaction between an ultrathin interface layer and the environmental surroundings, causing the formation of local pits on the nanoscale which give rise to further stress concentrations leading eventually to transgranular and intergranular cracking. The rupture of the protective layer also greatly facilitates the migration of embrittling species such as oxygen and chloride to new reactive zones in the material, the transport is again coupled to an evolving thermal, microstructural and stress environment. Thus, at the molecular scale, stress corrosion phenomena have their origins in the action of aggressive species in the interface layer with full environmental exposure.

One might ask what is known about the "passive" protective oxide film believed to be only a few nanometers in thickness. In the case of corrosion of iron, evidence from *ex situ* electron diffraction and electrochemical measurements suggest that this film is crystalline, consisting of an inner layer of $Fe_3O_4$ and an outer layer of $\gamma Fe_2O_3$. Later studies using *in situ* methods, such as Mössbauer spectroscopy, x-ray absorption fine structure, and surfaced enhanced Raman scattering show the film to be either amorphous or a spinel structure, a combination of $Fe_3O_4$ and $\gamma Fe_2O_3$ with stoichiometry of $AB_2O_4$, with A and B being divalent and trivalent cations respectively. Final resolution of this issue, based largely on *in situ* synchrotron diffraction, finds the film to be different from any bulk oxide phase [7]. Its structure, designated the LAMM phase, is crystalline [8], but also highly defective and may be regarded as that of a cation-deficient magnetite, $Fe_3O_4$. Moreover, the film is nanocrystalline, with grains of size 6 nm Fe(001) and 4.5 nm Fe(110).

Given the structure of the oxide layer the next question could be its microstructure evolution under conditions of temperature, stress, and reactive species. As we will see in Sec. III, part B, an attempt has been made to investigate ion transport in this system, but no definitive results are yet available. Thus any scenario of rupture remains future research. Modeling and simulation along with *in situ* spectroscopic and microscopic characterization approaches highlighted here present invaluable opportunities in elucidating governing mechanisms in the chemo-mechanical degradation of nuclear structural materials.

## 2. ATOMISTIC MEASURES OF STRENGTH AND TOUGHNESS

### 2.1 Multiscale Modeling and Simulation Capabilities

The emergence of multiscale materials modeling as a multidisciplinary outgrowth of computational science has received considerable recognition, as can be seen from a number of funding agency reports [9,10], collection of early conference proceedings and special journal issues [11,12] and compendium publications [13]. For illustrating the use of atomistic simulations to study structural stability, fracture, and defect transport properties of metals, we can point to a set of results on $\alpha$-Fe, ranging from early investigations of martensitic transformation [14,15] brittle-ductile transition in crack propagation [16-19], and grain-boundary diffusion [20,21] to more recent first-principles calculation of point defect concentrations in metastable Fe-C alloys [22], and the development of a many-body interatomic potential for Fe-C alloys [23]. These may be seen as examples of building a database of atomistic measures of strength and deformation in the attempt to understand materials strength at the microscale [24].

The mechanical stability of a crystal lattice can be defined through stability criteria, a set of conditions on the elastic moduli which specify the critical level of stress that the system can withstand [25,26]. This concept of ideal strength has been examined from the standpoint of elasticity [27,28], and extended to finite strain [29,30] and shown to be equivalent to a thermodynamic formulation by Gibbs [31]. As a consequence, we have now an understanding of how to determine theoretical limits to material strength using atomistic models and first-principles methods [32,33].

Under a uniform load the deformation of a single crystal is homogeneous up to the point of structural instability. For a cubic lattice under an applied hydrostatic stress, the load-dependent stability conditions are particularly simple, being of the form

$$B = (C_{11} + 2C_{12} + P)/3 > 0,\ G' = (C_{11} - C_{12} - 2P)/2 > 0,$$
$$G = C_{44} - P > 0, \quad (1)$$

where P is positive (negative) for compression (tension), and the elastic constants Cij are to be evaluated at the current state. Eq.(1) has a simple physical interpretation when one recognizes that B is an effective bulk modulus, and G' and G are the tetragonal and rhombohedral shear moduli respectively. While this result has been known for some time [34-36], direct verification against atomistic simulations showing that the criteria do accurately describe the critical value of P (Pc) at which the homogeneous lattice becomes unstable has been relatively recent [29,37-41]. One may therefore regard Pc as a definition of theoretical or ideal tensile (compressive) strength of the lattice.

Turning now to molecular dynamics simulations we

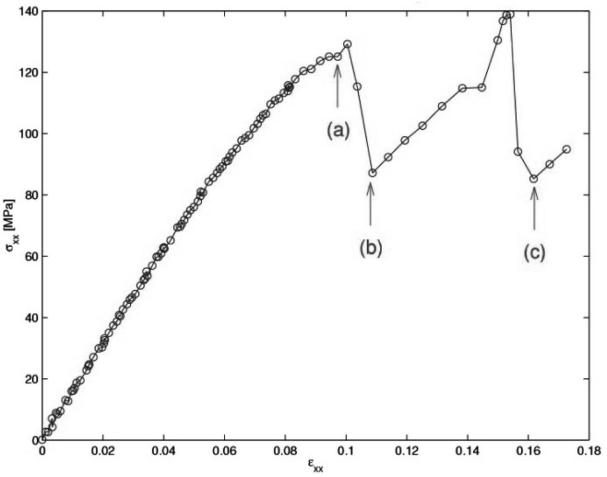


Fig. 1. Atomistic Stress-Strain Response of a Single Crystal of Ar Under Uniaxial Tensile Deformation at Constant Strain at a Reduced Temperature of 0.3 (35.9K). Simulated Data are Indicated as Circles and Solid Line is Drawn to Guide the Eye

show in Fig. 1 the stress-strain response for a single crystal of Ar under uniaxial tension at 35.9K [42]. At every step of fixed strain, the system is relaxed and the virial stress evaluated. One sees the expected linear elastic response at small strain up to about 0.05; thereafter the response is nonlinear but still elastic up to a critical strain of 0.1 and corresponding stress of 130 MPa. Applying a small increment strain beyond this point causes a dramatic stress reduction at point (b). Inspection of the atomic configurations at the indicated points shows the following. At point (a) several point defect like inhomogeneities have been formed; most probably one or more will act as nucleation sites for a larger defect which causes the strain energy to be abruptly released. At the cusp, point (b), one can clearly discern an elementary slip on an entire [111] plane, the process being so sudden that it is difficult to capture the intermediate configurations. Figuratively speaking, we suspect that a dislocation loop is spontaneously created on the (111) plane which expands at a high speed to join with other loops or inhomogeneities until it annihilates with itself on the opposite side of the periodic border of the simulation cell, leaving a stacking fault. As one increases the strain the lattice loads up again until another slip occurs. At (c) one finds that a different slip system is activated.

## 2.2 Microstructural Effects

Fig. 1 is a typical stress-strain response on which one can conduct very detailed analysis of the deformation mechanism using the atomic configurations available from the simulation. This atomic-level version of structure-property correlation can be even more insightful than the conventional macroscopic counterpart simply because in simulation the microstructure can be as well characterized as one desires. As an illustration we repeat the deformation simulation using as initial structures other atomic configurations which have some distinctive microstructural features. Consider the results on cubic SiC (3C or beta phase), which has zinc-blends structure, obtained using an empirical bond-order potential [43] for a single crystal and prepared amorphous and nanocrystalline structures. [44] Fig. 2 shows the stress-strain response to hydrostatic tension at 300K. At every step of fixed strain, the system is relaxed and the virial stress evaluated. Three simulation cells are studied, all with periodic boundary conditions. The amorphous sample is an enlargement of a smaller configuration produced by electronic-structure calculations [44]. The nanocrystal sample consists of four distinct grains with random orientations (7810 atoms). As in Fig. 1, the single-crystal sample shows the expected linear elastic response at small strain up to about 0.03; thereafter the response is nonlinear but still elastic up to a critical strain of 0.155 and corresponding stress of 38 GPa. Applying a small strain increment beyond this point causes a dramatic change with the internal stress suddenly dropping by a factor of 4. Inspection of the atomic configurations (not shown) reveals the nucleation of an elliptical microcrack in the lattice along the direction of maximum tension. With further strain increments the specimen deforms by strain localization around the crack with essentially no change in the system stress.

The responses of the amorphous and nanocrystal samples differ significantly from that of the single crystal. The former shows a broad peak, at about half the critical strain and stress, suggesting a much more gradual structural transition. Indeed, the deformed atomic configuration reveals channel-like decohesion at strain of 0.096 and stress 22 GPa. Another feature of the amorphous sample is that the response to other modes of deformation, uniaxial tension and shear, is much more isotropic relative to the single crystal, which is perhaps understandable with bonding in SiC being quite strongly covalent and therefore directionally dependent. For the nanocrystal, the critical strain and stress are similar to the amorphous phase, except that the instability effect is much more pronounced, qualitatively like that of the single crystal. The atomic configuration shows rather clearly the failure process to be intergranular decohesion. These observations allow one to correlate the qualitative behavior of the stress-strain responses with a gross feature of the system microstructure, namely, the local disorder (or free volume). This feature is of course completely absent in the single crystal, well distributed in the amorphous phase, and localized at the grain boundaries in the nanocrystal. The disorder can act as a nucleation site for structural instability, thereby causing a reduction of the critical stress and strain for failure. Once a site is activated, it will tend to link up with neighboring activated sites, thus giving rise to different behavior between the amorphous and nanocrystal samples.

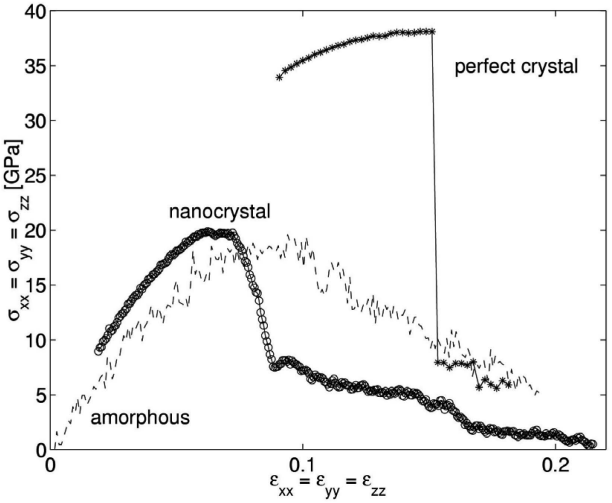


Fig. 2. Variation of Virial Stress at Constant Strain from MD Simulations of SiC (3C) under Hydrostatic Tension at 300K in Perfect Crystal, Amorphous, and NanocryStalline Phases

## 2.3 Crack front Extension: Fracture Fundamentals

Is it possible to study how a sharp crack evolves in a crystal lattice without actually driving the system to the point of instability? By this we mean following the pathway of crack front motion while the lattice resistance against such displacement is still finite. Despite a large number of molecular dynamics simulations on crack tip propagation (e.g., see [45]), this particular issue has not been examined. Most studies to date have been carried out in an essentially 2D setting, with periodic boundary condition imposed along the direction of the crack front. In such simulations the crack tip is sufficiently constrained that the natural response of the crack front cannot be investigated. Besides the size constraint on the crack front, there is also the problem that in direct MD simulation one frequently drives the system to instability, resulting in abrupt crack-tip displacements which make it difficult to characterize the slow crack growth by thermal activation. We discuss here an approach capable of probing crack front evolution without subjecting the system to critical loading. This involves using reaction pathway sampling to probe the minimum energy path (MEP) [46] for the crack front to advance by one atomic lattice spacing, while the imposed load on the system is below the critical threshold. This method has been used to characterize the atomistic configurations and energetics of crack extension in a metal (Cu) [47] and a semiconductor (Si) [48], allowing a comparison that elucidates how ductility or brittleness of the crystal lattice can manifest in the mechanics of crack front deformation at the nanoscale.

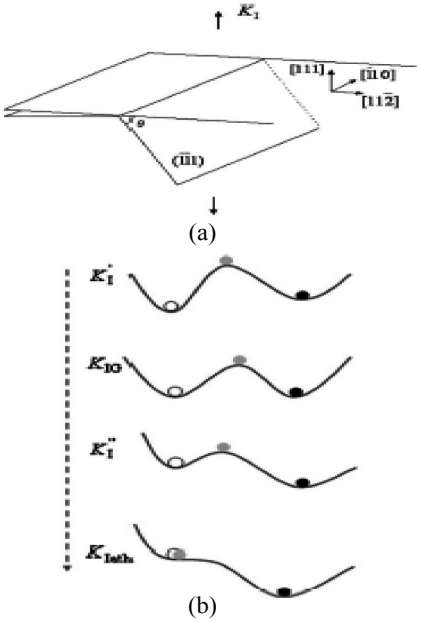


Fig. 3. (a) Schematic of a 3D Atomically Sharp Crack Front under a Mode-I (Uniaxial Tensile) Load K1, (b) Energy Landscape of the Crack System at Different Loads ($K'_1<K_{1G}<K''_1<K_{1ath}$). Open Circle Represents the Initial State of a Straight Crack Front under an Applied Load, Close Circle Denotes the Final State after the Crack Front has Uniformly Advanced by One Atomic Spacing (under the Same Load as the Initial State), and Shaded Circle Denotes the Saddle-Point [116]

Consider a 3D atomically sharp crack front which is initially straight, as shown in Fig. 3(a). Suppose we begin to apply a mode-I load in incremental steps. Initially the crack would not move spontaneously because the driving force is not sufficient to overcome the intrinsic lattice resistance. What does this mean? Imagine a final configuration, a replica of the initial configuration with the crack front translated by an atomic lattice spacing in the direction of the crack advancement. At low loads, e.g., $K_i'$ as shown in Fig. 3(b), the initial configuration (open circle) has a lower energy than the final configuration (closed circle). They are separated by an energy barrier which represents the intrinsic resistance of the lattice. As the loading increases, the crack will be driven toward the final configuration; one can regard the overall energy landscape as being tilted toward the final configuration with a corresponding reduction in the activation barrier (see the saddle-point states (shaded circle) in Fig. 3(b). As the load increases further the biasing becomes stronger. So long as the barrier remains finite the crack will not move out of its initial configuration without additional activation, such as thermal fluctuations. When the loading reaches the point where the lattice-resistance barrier disappears altogether, the crack is then unstable at the initial configuration; it will move without any thermal activation. This is the athermal load threshold, denoted by $K_{1ath}$ in Fig. 3(b). In our simulation, we study the situation where the applied load is below this threshold, thereby avoiding the problem of a fast moving crack that is usually over-driven.

The cracks in Cu and Si that we will compare are both semi-infinite cracks in a single crystal, with the crack front lying on a (111) plane and running along the ($\bar{1}$10) direction. The simulation cells consist of a cracked cylinder cut from the crack tip, with a radius of 80 A. The atoms located within 5 A of the outer surface are fixed according to a prescribed boundary condition, while all the remaining atoms are free to move. To probe the detailed deformation of the crack front, the simulation cell along the cylinder is taken to be as long as computationally feasible, 24 (Cu) and 2(Si) unit cells. A periodic boundary condition is imposed along this direction. With this setup, the number of atoms in the system are 103,920(Cu) and 77,200(Si). For interatomic potentials we use a many-body potential of the embedded atom method type for Cu [49] for which the unstable stacking energy has been fitted to the value of 158 mJ/m$^2$, given by an ab initio calculation, and a well-known three-body potential model for Si proposed by Stillinger and Weber [50].

Prior to applying reaction pathway sampling, we first determine the athermal energy release rate, denoted by

$G_{emit}$ (corresponding to $K_{Iath}$ in Fig. 3(b)).This is the critical value at which the activation energy barrier for dislocation nucleation vanishes, or equivalently a straight dislocation is emitted without thermal fluctuations [51,52].As detailed in [47], the athermal load is determined to be $K_{Iath}$ = 0.508Mpa$\sqrt{m}$(or $G_{emit}$ = 1.629J/m$^2$, based on the Stroh solution [53]) for the nucleation of a Shockley partial dislocation across the inclined slip plane. So long as the applied load is below $K_{Iemit}$ the crack front will remain stable. It is in such a state that we will probe the reaction pathway for dislocation using the method of nudged elastic band (NEB) [46]. The quantity we wish to determine is the minimum energy path (MEP) for the emission of a partial dislocation loop from an initially straight crack front. MEP is a series of atomic configurations connecting the initial and final states. Here the initial configuration is a crack front as prescribed by the Stroh solution which is then relaxed by energy minimization, while the final configuration is a fully formed straight Shockley partial dislocation, a state obtained by taking the simulation cell containing a pre-existing Shockley partial dislocation and reducing to the same load as the initial state.(The pre-existing partial was generated by loading the simulation cell at a level above the threshold $G_{emit}$.) To find the MEP a number of intermediate replicas of the system (15 in this case) which connect the initial and final states are constructed. We choose the intermediate replicas that contain embryonic loops resulting from the relaxation of a straight crack front, allowing for the nucleation of a curved dislocation. The relaxation of each replica is considered converged when the potential force vertical to the path is less than a prescribed value, taken to be 0.005 eV/A.

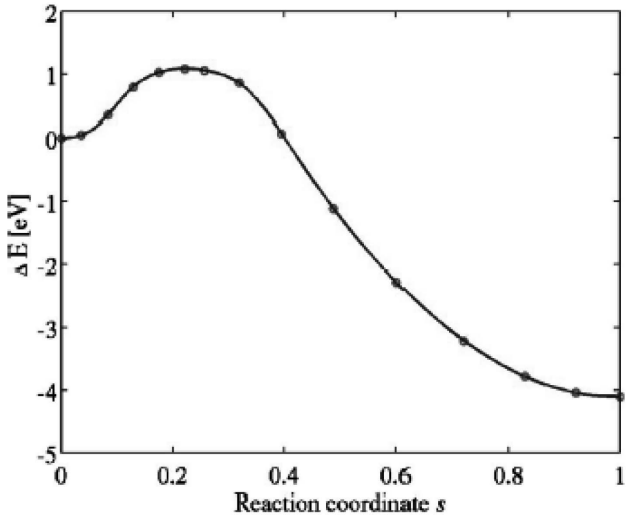


Fig. 4. MEP of Dislocation Loop Emission in Cu at a Load of G = 0.75$G_{emit}$ [47]

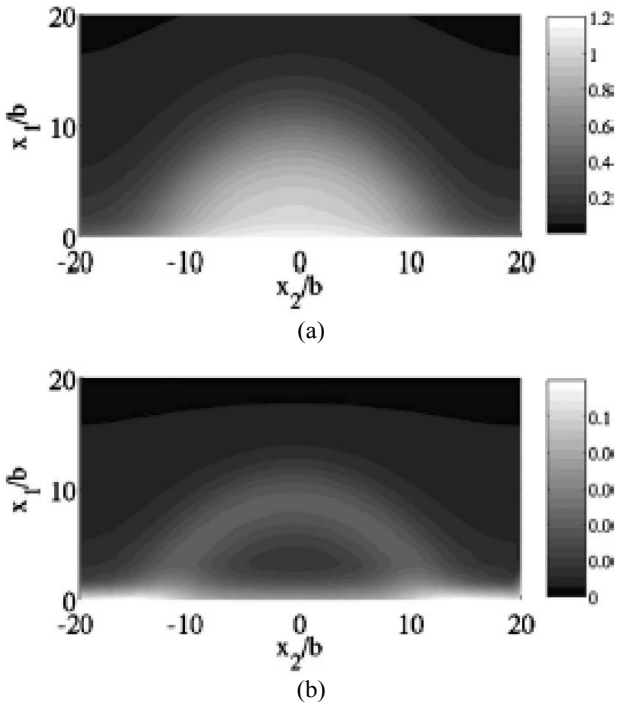


Fig. 5. Shear (a) and Opening (b) Displacement Contours across the Slip Plane at the Saddle-Point State [116]

The sequence of replicas define a reaction coordinate in the following sense .Each replica in the sequence is a specific configuration in 3N configuration hyperspace, where N is the number of movable atoms in the simulation. For each replica we calculate the hyperspace arc length $l$ between the initial state $\mathbf{x}_i^{3N}$ and the state of the replica $\mathbf{x}^{3N}$. The normalized reaction coordinate s is defined to be $s \equiv l/l_f$, where $l_f$ denotes the hyperspace arc length between the initial and final states. The relaxed energy of any replica is a local minimum within a 3N-1 hyperplane vertical to the path. By definition MEP is a path that begins at $\Delta E$=0($s$=0), where $\Delta E$ is the relaxed energy measured relative to the energy of the initial state. Along the path (reaction coordinate $s$) $\Delta E$ will vary. The state with the highest energy on this path is the saddle point, and the activation energy barrier is the energy difference between the saddle point and the initial state. Fig. 4 shows the MEP for the nucleation of a dislocation loop from the crack front in Cu, loaded at G = 0.75 $G_{emit}$. Notice that at this loading the final state is strongly favored over the initial state. The presence of a lattice resistance barrier at this particular loading is clearly indicated.

To visualize the variation of atomic configurations along the MEP, we turn to displacement distributions between atomic pairs across the slip plane. Fig. 5(a) shows a contour plot of the shear displacement distribution along the crack front at the saddle-point state. One can see the shape of a dislocation loop bowing out; the profile of b/2

shear displacement is a reasonable representation of the locus of dislocation core. Also this is an indication that the enclosed portion of the crack front has been swept by the Shockley partial dislocation loop. Besides shear displacement, normal or opening displacement, in the direction is also of interest. The corresponding distribution is shown in Fig. 5(b). One sees that large displacements are not at the center of the crack front. In Figs. 5(a) and 5(b) we have a detailed visualization of the crack front evolution in three dimensions. The largest displacements are indeed along the crack front, but they are not of the same character. The atoms move in a shear mode in the central region, and in an opening mode on the two sides. For a similar discussion of crack advancement in a semiconductor (Si) rather than a metal, the reader can consult [48].

## 3. CHEMO-MECHANICAL ISSUES IN SCC FUNDAMENTALS: SIMULATION PERSPECTIVE

There are many questions of a chemo-mechanical nature in the quantitative understanding of the breakdown of the oxide interlayer. To motivate our simulation perspective, we might start with a very simple notion - bond rupture as the initiation event leading to the mechanical failure in a system of atoms. Less recognized but no less valid is that bond strain also fundamentally affects the chemical reactivity of the atoms involved in the bonding. This dual role of bond strain is best examined when simulations can deal with rupture and reactivity on equal footing. We highlight four issues which are particularly appropriate for the present discussion. The first illustrates the role of electronic-structure calculations in dealing with chemical reactivity and electron transfer processes. The second concerns the modeling of cation transport which gives rise to a build-up of vacancy clusters. The third is the modeling of microstructural evolution in the oxide layer, specifically vacancy coalescence leading to pit nucleation. The last discussion extends the role of sub-oxide pits to the grain boundaries in the context of intergranular initiation and progression of corrosion under strain states, and elaborates on the development and use of *ab inito*-driven atomistic simulations in this context.

### 3.1 Chemical Reactivity and Electron Transfer

Modeling chemical reactivity in stress corrosion cracking (SCC) requires electronic-structure approaches capable of treating electron-transfer reactions [54] and describing accurately the chemistry of transition-metal complexes [55]. The techniques and algorithms also must consider complex boundary conditions to allow reactions occurring in solution [56]. We consider briefly a method for describing transition metals, based on the formalism of self-consistent, linear-response GGA+U, and a new energy functional for electron transfer processes.

#### *3.1.1 Self-Consistent, Linear Response GGA+U*

Though density functional theory (DFT) is exact in principle, the explicit expression of the exchange-correlation energy functional is not known and therefore approximations are needed. The most popular are the local-density approximation (LDA), in which the energy functional is that of a homogeneous electron gas with the same local charge density, and the generalized-gradient approximation (GGA), in which a measure of non-locality is introduced. The approximations are in the spirit of a mean-field approach, where each electron interacts with the charge density of the others. However, when the valence electrons are localized in atomic-like orbitals, their motion becomes correlated and many-body effects become dominant, as is the case for many transition-metal oxides. For these systems, most commonly used approximations can fail in a severe manner, for example, insulators are predicted to be metals and structural properties incorrectly calculated. Among the correction schemes that have been introduced the LDA+U approach is one of the simplest and most effective. One can introduce a modified form in which the strength of the correction is controlled by a screened on-site electron-electron repulsion $U$ ("Hubbard U") whose explicit expression and appropriate value now need to be determined [55]. This approach has been found to be effective in a study of the $Fe_2^-$ and $Fe_2^-$ dimers [55].

#### *3.1.2 Electron-Transfer and Redox Reactions*

According to the picture pioneered by R. Marcus, in a polar solvent the electron transfer process is mediated by thermal fluctuations of the solvent molecules. In the reactant state, the electron being transferred is initially trapped at the donor site by solvent polarization, but transfer can occur when the electron donor and acceptor sites become degenerate due to the thermal fluctuations of the solvent molecules. To characterize the role of the solvent on the electron-transfer reaction, a reaction coordinate for a given ionic configuration can be introduced as the energy difference between the product and reactant states at that configuration. This definition of reaction coordinate captures the collective contributions from the solvent [54].

It is important to note that self-interaction correction is lacking in common exchange-correlation functionals. Thus, the transferring (*3d* minority spin) electron will split between the two ions creating an unphysical condition. Moreover, to calculate the energy gap, we need to accurately calculate the total energy when the minority spin electron localizes at either reactant or product site at any given ionic configuration. The self-interaction failure is essentially a non-local problem. The Hartree self-interaction will split an electron whenever sites with comparable energy are available. A clear example of this failure is given by the case of two identical ions in

different oxidation states, such as the ferrous and ferric ion. Studying these in the same unit cell (or in the same simulation, if periodic boundary conditions are not used) will lead to an incorrect and unphysical splitting of the charge, with both ions in the 2.5 oxidation state.

This failure can be corrected by adding a penalty cost to the ground states with non-integer occupation of the ion centers. The same approach is also used to calculate the energy gap, where for a given configuration we need to determine both the correct ground-state energy (with the transferring electron in the reactant electronic configuration) and the first excited state (with the transferring electron in the product electronic configuration). This has been validated by calculating the energy gap using two different penalty-functional calculations imposing on the HOMO electron to localize first on one, then on the other ion. The four calculations involve $Fe^{2+}$ in two $Fe(H_2O)_6$ geometries (A and B), and $Fe^{3+}$ in the same geometries. The energy gaps we obtained with the penalty functional are 0.632, 0.569, 0.769 and 1.027 eV, which agree well with the "4-point" values of 0.622, 0.542, 0.769 and 1.012 eV. With these tools, we have determined the diabatic free energy surfaces for two iron ions separated by 5.5 Å and solvated in 62 water molecules, in periodic boundary conditions. The reorganization energy obtained is 2.0 eV , while the experimental value is 2.1 eV. The energy barrier is 0.49 eV, about a quarter of the reorganization energy, as expected.

### 3.2 Cation Transport

Returning to the passive film on iron discussed in the Introduction, an attempt has been made to calculate the atomic structure by applying first-principles methods involving density functional theory and approximations for the exchange and correlation functional [57]. In this approach one determines the energetics and the electronic structure of the cation interstitials and vacancies and the interrelationships between site occupancies. The results of the total-energy pseudopotential calculations using DFT-GGA show the film to be metastable relative to the iron substrate, and reveal significant correlation between the octahedral interstitials and tetrahedral vacancies which is consistent with the cation deficiency of the LAMM phase [57]. Having access to activation energy barriers for various charged defects enables this first-principles study to come up with new insights that can be further pursued. Thus, comparing the energy barrier of 0.88 eV for cation migration through the tetrahedral sublattice with 1.3 eV for migration through the octahedral sublattice, one can conclude that tetrahedral interstitials are likely to play an important role in cation transport in the passive film. This could be a useful point of view from which one can try to understand the processes leading to film breakdown, as will be discussed below.

The advantage of a molecular description of the passive film is that one can go well beyond understanding the structure of the interface [57]. Hendy et al. [58] have exploited this capability by following up on their first-principles description of the atomic and electronic structure of the prototype Fe film. They have recently initiated atomistic modeling of cation transport in which they leveraged on their previous DFT-GGA calculations and the insights from a considerable literature on modeling efforts on the growth kinetics of the interface. By considering the same prototype passive film on which they have already invested appreciable efforts they are able to compute activation energy barriers for specific migration paths of the relevant charged defects, and use the results to test the consistency of various growth models that have been proposed. This is a good example of how results predicted by a molecular model can be used to confront existing growth models which invariably involve adjustable parameters derived by fitting experiments. In other words, the model based on first principles provides a different set of kinetics data for validating the existing more empirical models. This is one way to make use of the molecular description. Another would be to make predictions to directly compare with experiments. In the case of film breakdown, the former route is taken because there are few precise measurements at the molecular level that are available for explicit comparisons. Most relevant data tend to be of an integral nature that an intermediate model is needed to connect with the molecular-level results. This issue becomes even more challenging when new factors of complexity enter into the study, not only from iron to Fe-based alloys, but also the addition of environmental effects such as radiation damage.

The use of first-principles methods to study cation transport in the passive film on iron is a pioneering attempt [58]. Although the treatment used is not the most definitive possible, one can see very well from this experience the different aspects of complexity that come into play. For the LAMM phase discussed above, Hendy et al. have analyzed two cation migration pathways mediated by defect mobilities through vacancies in the tetrahedral and octahedral sublattices by applying a transition-state pathway sampling procedure (Nudged Elastic Band) to estimate the corresponding diffusion coefficient [58]. Using the results to constrain parameters in several existing models of growth kinetics they did not find consistency with the high-field model [59] or the diffusion-limited model [60]. However, the tests are not conclusive because these models assume the film is homogeneous.

Cation transport, by vacancy diffusion for example, is fundamental to both passive film growth and film breakdown [61]. The diffusion of charged defects in mixed valence oxides is a very complex problem not yet fully explored at the first-principles level. This is because in addition to the local bonding chemistry, diffusion is also affected by global factors such as the electric field, stress field and the electronic Fermi energy. It is known that the formation energy of a charged defect depends on the electronic Fermi energy relative to band edges [62],

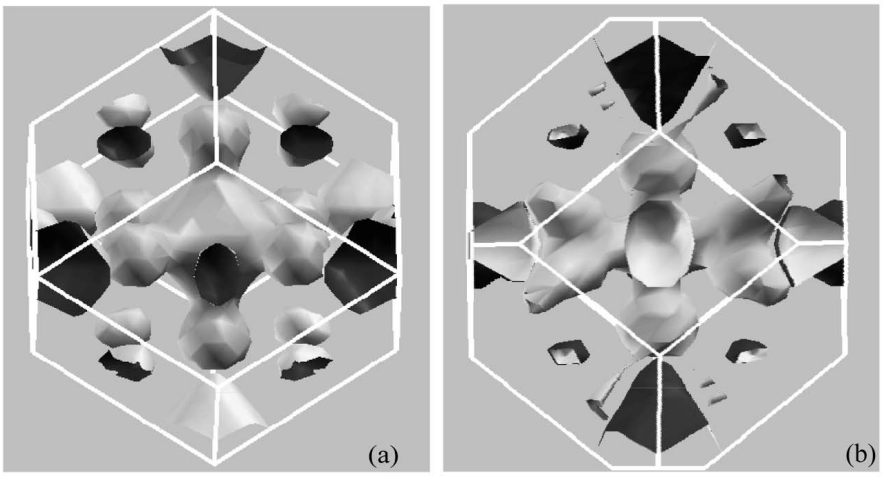


Fig. 6. Shape of the Calculated Fermi Surface in bcc Cr, (a) Unstrained, (b) 10% Strained Axially along <001> Direction. Grey: Electons, White: Holes, Black: Inside the Electronic and Hole Density Surfaces, Pink: Overlapping Density Cross Sections

and a switching in the defect's charge state will occur when the Fermi energy is altered due to doping and/or introduction of additional interfacial charging states. To illustrate this visually, we present the calculated Fermi surface for Cr as a function of strain in Fig. 6 from our ongoing work. The first-principles analysis is being conducted within the framework of density functional theory using Plane Wave self-consistent field (PWscf) method with Generalized Gradient Approximation pseudopotential as implemented in QuantumEspresso (QE) [63] computational software package. The investigation of the electronic structure and bonding characteristics during mechanical deformation in the presence of tensile or/and shear stress can reveal the mechanism of the deformation, as well as corrosion under strain conditions. In this simulation example, before the strain was applied, the Fermi surface of the bulk BCC Cr shows highly symmetric shape which is consistent with the previous experimental results [64]. The strained surface on Fig. 6-b corresponds axially to <001> direction. As can be observed, the applied large strain, 10%, disturbs the symmetry resulting in splitting of the electron knobs and significant decrease in the size of the hole pockets. The Fermi energy increases as the applied strain increases. Such changes in Fermi energy and the shape of Fermi surface will affect the mechanism of oxygen reaction with the surface in the initiation of corrosion, as well as metal cation and oxygen anion transport at interfaces.

The Fermi energy of a realistic oxide structure with phase boundaries, grain boundaries and point defects must be determined by solving a global problem of electro-negativity equalization, the continuum version of which is the Poisson-Fermi equation frequently employed in semiconductor device modeling and processing. However, the spatial resolution of a continuum model could be insufficient to describe oxide film of a few monolayers, with sharp microstructural features such as pits and interfaces. Direct DFT modeling, on the other hand, is infeasible to describe all the necessary geometries that can impact on the diffusion barrier through electric field and electronic Fermi energy.

### 3.3 Passive Film Breakdown: Microstructure Modeling

While metal dissolution is greatly reduced by the protective oxide film, the film surface itself is susceptible to various forms of localized attack, such as pitting, stress corrosion cracking, corrosion fatigue and crevice corrosion. These phenomena all involve the rupturing of the interface layer causing the underlying metal to be exposed to the environment. Generally speaking, localized corrosion occurs in a wide variety of metals in many different kinds of environments, the initiation sites typically being structural and chemical discontinuities. Pit nucleation is a rare event, with probability of surviving the metastable growth stage of the order of $10^{-2}$ - $10^{-5}$, and its stability depends on many factors in repassivation. Numerous theories and models have been proposed to describe this breakdown [61]. It is fair to say that no single model is adequate for the purpose we have in mind - provide a quantitative basis for the investigation of passive film breakdown. On the other hand, the Point Defect Model (PDM), which postulates that film breakdown is a result of cation vacancy condensation [61], is a reasonable physical model in which to frame the questions for microstructure modeling and simulation. In the PDM scenario pit nucleation occurs when sufficient cation vacancies accumulate at film/metal interface to initiate

local film detachment from the metal which in turn leads to film perforation and rupture. Once a pit is nucleated, new metal is exposed. Thus the pit may be stabilized by repassivation or it can undergo stable growth.

The injection of vacancies at the interface by cation diffusion has been demonstrated by direct observation of chemical and structural modifications of the topmost layers on atomically smooth substrate surfaces [65]. This was achieved by x-ray photoelectron spectra and STM measurements during the very early stage of growth of the oxide film on an intermetallic alloy TiAl. The atomic vacancies were found to aggregate to form nanocavities.

### 3.3.1 Microstructural Modeling of Passivity Breakdown

Electronic structure calculations will provide essential information regarding atomic structures of the oxide layers [57], cation mobility under electric fields [58], effects of solution chemistry such as halide ions, etc. However, there are also larger length-scale issues that critically influence passivity breakdown [61,66-68]. How corrosion pits are nucleated, their stabilization versus repassivation, the spatial and temporal correlations of these pits reflecting their interactions [68], and crevice and crack developments are complex issues that involve stress buildup and establishment of chemical concentrations in the solution and oxides on ion diffusion timescales. The goal of microstructural modeling is to realistically account for the structural complexities of the oxide layer, if necessary with atomic resolution, and relating them to the kinetics of passivity breakdown.

Passivity breakdown is a runaway instability that at the most basic level is no different from crack propagation or shear localization [69], in that a strong field is established due to very large local gradients which greatly amplify free energy reduction. A starting point could be to combine analytical modeling, numerical PDE solutions and atomistic modeling to investigate microstructural effects on pitting corrosion and cracking. Local stress dependent rate laws could be calibrated against *ab initio* calculations following a chemo-mechanical coupling scheme introduced by [70]. Atomic-scale transitions such as cation dissolution and vacancy hop and condensation will be expressed in Arrhenius form, $R=e^{-Q(\sigma)/kT}$, where $Q(\sigma)$ is the activation free energy of forward or backward reactions. $Q(\sigma)$ will be modeled by a first order expansion, $Q(\sigma)=Q(0)-T\gamma(\sigma\Omega)$, where $\Omega$ is a tensorial activation volume. It has been shown recently that $\sigma$ can be computed atomistically [24,71]; for point-defect processes these can be deduced from *ab initio* calculations. Such stress dependent kinetics will be an advance over previous fixed-grid kMC models with fixed rate constants [72].

An interesting example we present here is from the passivity breakdown on aluminum alloys [73]. Corrosion resistance of aluminum alloys is related to the presence of a thin, passivating aluminum oxide film on the surface. Rashkeev and co-workers performed first-principles quantum-mechanical calculations to provide atomic scale understanding of the initiation of corrosion in Al. They particularly investigated the interaction between hydrogen and defects in alumina and at $Al/Al_2O_3$ interfaces. Their results showed that atomic hydrogen can migrate from the oxide surface into the alumina film. An accumulation of several hydrogen atoms within a cation vacancy was energetically favorable and tended to break the bonds between the surrounding atoms thus initiating void formation in the form of hydrogen blisters formation within the oxide film as well as at the interface between the oxide and the Al metal, as shown in Fig. 7. The corrosion is then initiated by a breakdown of the oxide film and a subsequent pit development on the surface of the metal exposed to the environment. The structural

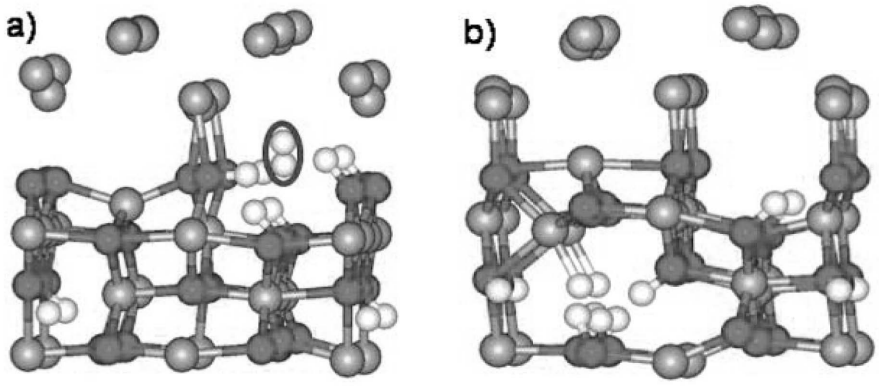


Fig. 7. Structural Damage Caused by Several Hydrogen Atoms Introduced (a) at a "Defect Free" Al/$\gamma$-Alumina Interface and (b) in the Tetrahedral Vacancy Nearest to the Interface. The Black Ellipse Highlights the Formation of a H2 Molecule in the Interfacial Region, as a Possible Precursor for a Hydrogen Blister. Figure is Taken from [73]

damage at the Al/alumina interface was significantly enhanced when interfacial mismatch defects are present. These results provide an atomistic picture of the initiation of the corrosion in aluminum, and provides motivation for similar studies in the investigation of passivity breakdown on nuclear structural metals.

### 3.4 Intergranular Initiation and Progression of SCC

In addition to pit formation and general dissolution of the surface, as detailed in the previous sections, the interface passive layer can also be destabilized owing to the chemical or physical deformation of the grain boundaries [74,75]. This would lead to intergranular progression of corrosion, oxide penetration and embrittlement. Grain boundary deformation can arise from the segregation or depletion of alloy or impurity components and the interaction of defects with the grain boundaries. These phenomena cause breakage of interatomic bonds in the initiation and propagation of intergranular cracks, which lead to further oxidation of the alloy along the grain boundary beneath the oxide layer. Particularly Cr-containing Fe-base and Ni-base alloys show susceptibility to the intergranular progression of stress corrosion cracking in oxidizing environments. In reality, no one alloy or microstructure has been found that can adequately endure both intergranular stress corrosion cracking and irradiation induced chemical and structural changes in the grain boundaries. A tremendous opportunity to provide advances in materials properties could arise from tuning the interface properties of alloys using tailored microstructures against intergranular chemo-mechanical degradation. Realization of this opportunity requires fundamental understanding and correctly tailoring of the microchemical and structural properties associated with the interfaces of alloys, namely their surfaces and grain boundaries. Again, fundamental computational approaches are essential in providing a predictive understanding the molecular-level characteristics of, in particular, interface reactive transport, and such enabling new knowledge is critical to designing high-performance alloy microsctructures for the present and future nuclear reactors.

Numerous experimental studies on the mechanism of oxidation, corrosion, and stress corrosion cracking of light water reactor components as functions of alloy microstructures and microchemistries [74,76,77] have shown several important phenomena taking place at the grain boundaries that influence the intergranular failure of the alloy: segregation of solutes and impurities at the interfaces, diffusion of oxygen and solutes along the grain boundaries, interaction of defect networks with the grain boundaries, and the stress at the grain boundary. Especially, Cr-depletion near the grain boundaries was found to directly relate to the corrosion and SCC mechanisms on steam generator tubing, nuclear fuel cladding, and pipes. Furthermore, recent experimental studies [75,76] have shown that the corrosion resistance of various alloys under oxidizing conditions can be significantly affected by the grain boundary structure, namely its texture, misorientation angle and coincident site lattice (CSL) fraction. Thus, tailoring the grain boundary structures and controlling the population of special grain boundaries in the alloy microstructure gives the opportunity to improve the corrosion resistance of alloys in extreme environments. The high resistance of special grain boundaries (such as CSL-type and low-angle grain boundaries) to intergranular corrosion and cracking is thought to be due to their highly ordered structure altering the diffusion, their lower energy, and their greater ability to resist deformation [78]. Furthermore, grain boundary structure also influences the grain boundary composition through altered segregation of alloying elements and impurities, particularly of Cr [79]. Therefore, the grain boundary structure-dependent interfacial microchemistry and mechanical properties are expected to play an important role in the thermodynamic and kinetic aspects of the alloy's intergranular corrosion and SCC. However, there is no prior work that elucidates the fundamental relations of the grain boundary structure to the interface chemistry, oxidation and cracking mechanism in Fe/Cr alloys, especially for nuclear reactor materials.

There is a need to obtain an analytical and predictive understanding of the relations among corrosion in oxidizing environment, and the chemical, physical, and structural properties of the alloy grain boundaries. In accomplishing this objective, the use of *ab initio* and atomistic simulations in an integrated way, and coupled to experimental validation is essential. The results of this investigation can provide the new knowledge needed for molecular-level tailoring of the grain boundary structural and compositional properties to decrease susceptibility to intergranular SCC in Fe/Cr steels.

Three categories of atomic configurations at the grain boundary [80,81] of model Fe/Cr interfaces can be considered: low angle, coincident site, and high-angle. At these interfaces, the predecessor mechanisms of mechanical failure under chemically reacting conditions are: structure, irradiation, and strain-driven deterioration of the interface composition, diffusion of oxygen, Cr and Fe long and across the interfaces under local strain, and the charge transfer reactivity of the interface to oxidation and corrosion under local strain. For a range of local stresses, it is important to identify the favorable structures and compositions at the grain boundaries that suppress the corrosion and mechanical failure.

The chemical reactivity of the interfaces is best handled by quantum mechanics. This is valid both for the chemical reactions with oxygen at the interfaces, as well as the interface composition that may be driven either by surface energies or by other competing factors. For example, the interface Cr concentration for a given bulk Fe-Cr composition is affected not only by the interface energies, but also by the ferromagnetic ordering of Fe and the

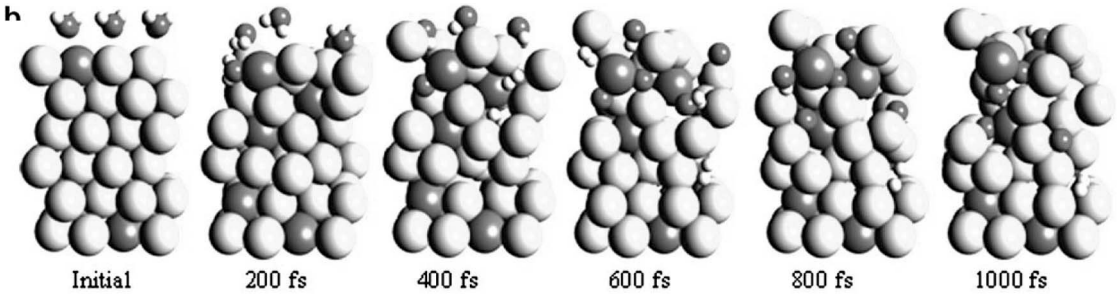


Fig. 8. Time Evolution of Surface Morphologies on Fe-Cr (111), with 1% Strain, During Water Dissociation and Transport into Fe-Cr at the Initiation of Corrosion. Figure Taken from [88]

antiferromagnetic ordering of Cr [82]. For the first time, Ropo et al. demonstrated by simulations that the surface chemistry of Fe-Cr alloys follows the experimentally observed peculiar threshold behavior characteristic of ferritic stainless steels. They showed that in dilute alloys the surfaces are covered exclusively by Fe, whereas for bulk Cr concentration above 10% the Cr-containing surfaces become favorable. The two dissimilar regimes of the surface compositions were explained based on the magnetic frustration of Cr, segregating in Cr-rich clusters, including at the surfaces. Their ability to address this problem at a first-principles quantum-mechanical level has become possible through the exact muffin-tin orbital (EMTO) method [83] based on density functional theory [84] in combination with the generalized gradient approximation [85]. This approach has proved to be an accurate tool in the theoretical description of Fe-based random alloys [86,87]. Considering the abrupt changes in the electronic density at the interfaces, surfaces as well as grain boundaries, segregation or depletion of Cr at the grain boundaries in the context of SCC should also be carefully considered at the quantum-mechanical level.

The work of Kumar Das et al. [88] is one of the first papers to describe the Fe-Cr surface in an oxidizing environment of high temperature water in the presence of strain, using quantum chemical molecular dynamics (QCMD) accounting for both the dynamical processes and electronic structure. The authors aimed to describe relation between strain and oxidation for both regular and defected surfaces of Fe-Cr as well as pure Fe. The method for electronic structure calculation includes Huckel approximation which is generally used to determine the energies and shapes of the p molecular orbitals. In the Molecular Dynamics part of the code, the Verlet algorithm was employed with NVT ensemble. The temperature was controlled through the atom velocities. Two important results from this work are worth presenting here: 1) Surface morphologies (Fig.8) differ from Fe to Fe-Cr because of strong bond between oxygen and chromium atoms. Oxygen atoms were trapped around chromium atoms at Fe-Cr surface, forming a Cr-rich protective oxide film, whereas oxygen penetrated into the lattice of Fe bare surface. In the presence of Cr, the oxygen diffusion into the Fe-Cr crystal surface was reduced. It indicated that the preferential oxidation of chromium would take place on Fe-Cr clean surface at the beginning of the oxidation process. 2) Strain was shown to enhance the dissociation of $H_2O$ molecules (Fig.8), accelerating the electron transfer in between the metallic and non metallic ions. In addition, diffusion of hydrogen and oxygen significantly increased when strain applied to the defective surface. Diffusion of hydrogen and oxygen significantly increased when strain applied to the defective surface. Enhanced penetration and weakening of metal bonding due to strain may play a role in localized corrosion and SCC. Results in this work are physically intuitive based on our accumulated knowledge from prior experimental observations. Nevertheless, this work has been an appreciable effort as the first quantum chemical description of the initiation of corrosion on Fe-Cr with ties to localized corrosion as SCC, and opens up new opportunities to utilize this approach for more detailed investigation of Fe-Cr interfaces in chemo-mechanical environments.

As seen in the examples above, addressing the interface chemical behavior in structural metals, including Fe-Cr, at a first-principles quantum-mechanical level based will be of essence to provide predictive understanding of the complexity of interface segregation, diffusion, bond breaking and construction in oxidation and corrosion, under strain conditions. However, mechanical failure dynamics propagating along the grain boundary calls for simulations including long grain boundary paths and the bulk of the grains, which involve larger temporal and spatial scales than the practical limits of DFT. To extend the length and time scales of interest in such studies beyond that of DFT, integration of the DFT results with atomistic scale simulations are needed. Such coupled quantum-atomistic approaches have been developed and employed, for example, to gain a comprehensive understanding of the energetics, kinetics, and dynamics

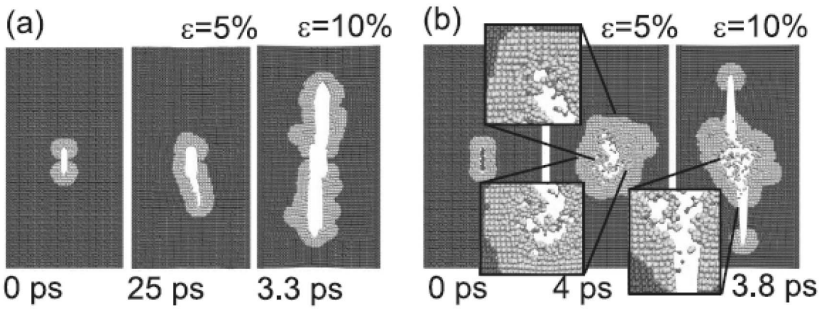


Fig. 9. Crack Dynamics in Silicon without (a) and with $O_2$ Molecules (b). Figure Taken from [92]. The Gray Regions are Tersoff Atoms, whereas the Colored Regions Correspond to ReaxFF Atoms. The Cracks in Si with $O_2$ Environment are Blunted Compared to the Sharp Cracks in pure Silicon without $O_2$ Molecules. Figure from [92]

of chemical processes involving surfaces and interfaces of hard materials. The idea here is to incorporate the precision of *ab initio* calculations into the larger scale capabilities of molecular dynamics simulations, in an "*ab initio*-driven molecular dynamics, AIMD" approach [89] which retains the true time evolution. A starting point could be developing new classical potentials to capture the interface behavior from *ab-inito* simulations, for example for the interactions of Fe, Cr, O, and H with each other for various states at the Fe-Cr interface. Then one can bring the molecular dynamics to bear upon the problem of including the chemically and spatially evolving interfaces into larger scale simulations. The availability of quantum mechanical information for various states allows one to increase or decrease the complexity of a potential and thereby ascertain the importance of different physical effects. For covalently bonded materials, Goddard and co-workers [90,91] developed reactive potentials (referred to as ReaxFF for "reactive force field") fit to data sets derived from ab initio calculations on clusters and condensed phases. The key in this approach will be the ability to handle bond formation and breaking at the interfaces, albeit more approximately than true *ab initio* methods. A successful application of this approach was shown by Buehler et al. [92] for the bond breaking and crack propagation in silicon. This study has shown that the crack behavior in pure silicon differs from that of silicon in the presence of oxidation (Fig.9), and similar phenomena can as well be expected for structural metals. In the case of structural metals, while the bulk behavior can be appropriately handled by MD using classical potential, for example the recently developed EAM model by [93-95] for Fe-Cr, there is no prior work in developing and implementing AIMD methods for the interfaces in reactive and mechanically loaded conditions. Thus, a great opportunity exists in developing large scale predictive simulation capabilities using AIMD approaches for the Fe-Cr interfaces in chemo-mechanical degradation conditions.

## 4. *IN SITU* EXPERIMENTAL INVESTIGATIONS OF THE EARLY STAGES OF CORROSION

There have been numerous studies on the mechanism of oxidation, corrosion, and stress corrosion cracking of light water reactor components as functions of alloy microstructures and microchemistries [74]. A large number of the corrosion failure studies have focused on experimental approaches such as *ex situ* microscopy [96], and *ex situ* synchrotron x-ray characterization [97-100]. These studies have provided a qualitative understanding of several phenomena taking place at the grain boundaries that influence the oxidation and intergranular failure of the alloy - for example, precipitation, segregation of alloying elements and impurities at the interfaces, diffusion of oxygen and alloy elements along the grain boundaries, interaction of defect networks with the grain boundaries, and the stress and stacking fault energy at the grain boundary. Especially, Cr-depletion near the grain boundaries was found to be directly related to the corrosion and IGSCC mechanisms in relation to SCC on the primary-side of PWR steam generator tubing, PWR cladding, and BWR pipes. However, yet little is known experimentally about the fundamental correlations of the surface chemistry, the initiation and progress of oxidation, pitting, and corrosion, and the evolution of interfacial stresses in the oxide and base alloy in high temperature and high pressure conditions. These factors necessarily must be studied in the corrosion environment, which makes the experimental probing of particular interfaces difficult especially when high pressures are involved. Therefore, there is a tremendous opportunity to shed new light on these issues through new capabilities for *in situ* studies of interfacial chemistry, structural evolution, and oxide growth strains. Furthermore, we envision that the *in situ* spectroscopic and microscopic characterization be used in direct information exchange with the simulation approaches we present in this paper. In this section, we highlight here the opportunities for the use of *in situ* synchrotron x-ray characterization, as well

as *in situ* scanning probe techniques for studying the general and localized corrosion. While the laterally averaged surface state can be probed by x-rays, the role of surface defects in the initiation of corrosion, the electronic and topological structure of the oxide as a function of inhomogeneities can best be probed by high resolution scanning probe techniques.

### 4.1 X-ray Techniques for Probing the Oxide Film Formation and Growth

A range of advanced synchrotron x-ray techniques, based on scattering or spectroscopic methods, are available for *in-situ* characterization of the metal surfaces, and the oxide layers at the initiation and progression stages. The most important parameters that can be measured in order to couple to the simulations discussed in this paper are the oxidation states and electronic structures at the interface, and the crystal structure and the strain state of the oxide layer during its growth.

The main advantage of using x-ray techniques for the chemo-mechanical degradation at the fluid-metal interfaces stems from the unique characteristics of brilliant and high-energy synchrotron x-rays that can penetrate deeply without suffering from severe attenuation *and* provide sufficient sensitivity to the structures and chemical states of the surface and sub surface layers. While there are advanced techniques (as elaborated below) that make use of high energy x-rays and provide interface sensitivity, the information probed in such measurements would provide laterally averaged data, i.e. no explicit data on the distribution of inhomogeneities on the surface. In this case, x-rays must additionally penetrate window materials (e.g. diamond) that must withstand the pressure of a cell to accommodate the temperature and pressure conditions representative of the working fluid, e.g. 15MPa to simulate the PWR conditions, or upto ~25 MPa needed to reach the supercritical water condition.

Specular and off-specular x-ray reflectivity geometries in x-ray scattering can prove especially useful for or chemical, structural and morphological investigation of the oxide film formation. Specular reflectivity can be used to obtain structural information about the samples, such as film thickness and roughness of the oxide film [101]. Off-specular reflectivity can be used to identify morphological evolution, pit formation, and film breakage of the oxide films, as was shown for Cu under reducing and oxidizing potentials by You and coworkers [102-104]. For incident angles below the critical angle of total external reflection, the x-ray penetration depth is limited by exponentially decaying evanescent waves to a few to hundreds of nanometers, allowing us to control the depth at which x-ray can penetrate. Above the critical angle, x-ray penetration depth is limited by the absorption of x-rays through the alloys. In this case, the penetration depth is inversely proportional to the angle of incidence and the penetration depth increases to hundreds to thousands of nanometers. In both cases, the consequent penetration depth can easily be calculated from the well-known optical principles for x-rays. Therefore, a wide range of depth profiling from a few nm to many microns can be done by accurately controlling the incidence angle [105,106]. With the capability to control the depth-sensitivity of measurements the following information can be extracted *in situ* during the oxidation and corrosion of alloys in high temperature fluid environments:

(i) depth-sensitive grazing incidence x-ray diffraction (GIXRD) for near-surface and sub-surface oxide structures, and strain states. Using an area detector (image plates or CCD), we can record a complete powder diffraction pattern *at each depth*. Analysis of the powder intensity distribution enables us to measure depth-sensitive phases, textures, and interfacial strain distributions in various alloy phases as well as in the oxide films [97].

(ii) depth-sensitive absorption spectroscopy measurements, using x-ray energies matching the Fe, Ni, and Cr K-edge absorption energies, known as reflection x-ray absorption spectroscopy (reflXAS), for information about the oxidation state of the absorbing atom and its local electronic and chemical coordination environment [107]. The reflXAS technique is much like x-ray absorption near-edge structure (XANES) and extended x-ray absorption fine structure (EXAFS) [108], but specifically sensitive to surfaces, and appropriate for the constrained geometries expected for the high temperature and pressure corrosion cells.

A unique example in probing the oxide layer formation on austenitic steels in high temperature and high pressure water is presented by Yildiz and co-workers [109]. This effort has been the first-ever x-ray investigation of solid-fluid interfaces under high pressure and temperature (up to supercritical water) conditions demonstrating the depth-sensitive diffraction measurements during oxidation on the surface of the alloy in a high pressure microreactor cell [110]. Using these capabilities, the researchers have been able to follow the initial adsorbed layers and the oxide growth in SCW on two different materials, showing continuous, conformal oxide formation on both a Ni 200 alloy and stainless steel 304 (SS304). The powder diffraction pattern from the SS304 sample (Fig. 10) shows prominent austenite iron ($\gamma$-Fe) peaks as expected. When this sample was heated to 350°C at 25MPa (the green curve), new peaks appears in the diffraction pattern taken at low incidence angles (0.35°), which can be indexed to $Cr_2O_3$. Taken together with the reflectivity data, this suggests that a thin amorphous film first formed on the surface which then grew and became crystalline $Cr_2O_3$ at higher temperatures over several hours of our measurements. Chrome oxides are known to form protective films on austenite stainless steels in oxidizing conditions, [111,112] and thus, the observation in this work that $Cr_2O_3$ starts to form at subcritical water conditions fits well with other

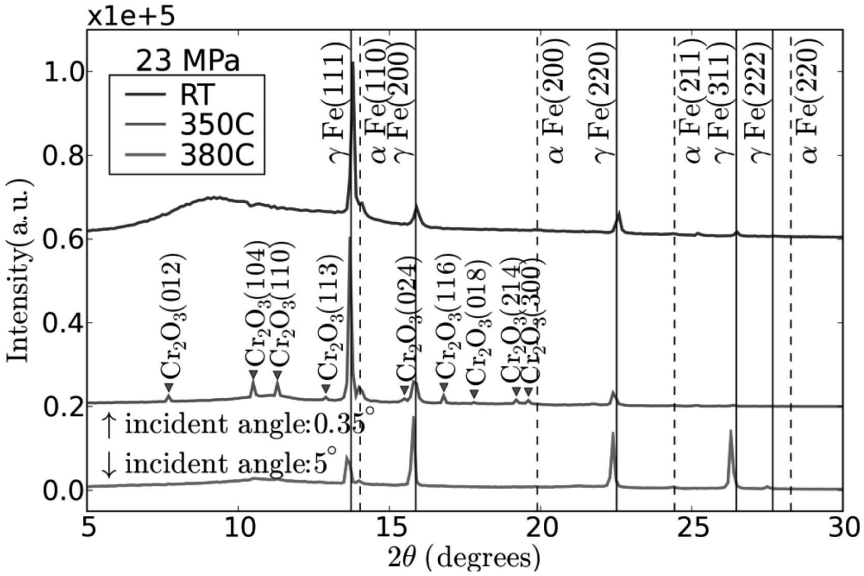


Fig. 10. X-ray Powder Diffraction of SS304 Alloy under High Pressure at Increasing Temperature

studies. The importance of the incidence angle of the x-ray is illustrated in the bottom pattern of Fig. 10. At high incidence angles probing subsurface region of ~10 microns (the incidence angle of 5°), the $\gamma$-Fe peaks were considerably favored around the (200) and (311) peaks as was the case for the Ni sample, indicating texturing along the cubic <100> direction; $Cr_2O_3$ peaks are nearly invisible. At the glancing angle (the incidence angle of 0.35°), we can see that the $\gamma$-Fe peaks are strongly favored at the (111) position indicating that the sample has a strong <111> texture for the near surface region (~10 nm thick).

Undoubtedly, further studies are needed for quantitative investigation of the layers present in the oxidized samples, and the sample configuration can be extended to one that accommodates mechanical load in addition to the chemically aggressive conditions. However, this illustration unambiguously demonstrates and motivates that the x-ray incidence angle can be varied to increase the sensitivity of the measurement to the top layers of the sample, allowing to do depth profiling under *in situ* condition of high temperature and pressure conditions, using the high-energy, high-brilliance hard x-rays available at synchrotron beam lines.

## 4.2 Scanning Probe Microscopy and Spectroscopy of Surfaces in Corrosion

The progress of microscopy within the last decades has shown that by investigating a surface at a higher magnification, some pitting can be correlated with surface heterogeneities in corrosion. Techniques such as electron microscopy and optical microscopy were used to examine the surface morphology of stainless steel (inclusions, precipitates, grains boundaries) before and after corrosion. In addition, AES, XPS or EDX are used to characterize the chemical nature of the surface, but, with exception of optical microscopy which has poor resolution [113], *in situ* observations are not accessible. The uprising of scanning probe micrsocopy in the late 90's, especially atomic force microscopy (AFM) and its derivative scanning Kelvin probe force microscopy (SKPFM), and scanning tunneling microscopy and spectroscopy (STM, STS), have enabled *in situ* observations of corrosion reactions on metal surfaces with very high resolutions [114].

While the AFM can enable a visual correlation of the structural inhomogeneities, such as grain boundaries, with the onset of pitting, SKFPM and STS can allow to identify the local electronic behavior of the alloy surface, adsorbed oxide layer, and growing oxide layers. The interface work function, band gap, and valance and conduction band structures can then be related to the electron transfer and oxygen exchange reactions on the metal and oxide interfaces, grain boundaries, pits, and impurities. Performing the scanning probe microscopy and spectroscopy measurements at the *initiation* of oxidation and corrosion under controlled oxygen environments and temperatures can become an invaluable tool for understanding the electron exchange reactions. Furthermore, this would be a critical point for information exchange between experiments and simulations at the first principles levels.

To our knowledge, while there is a large volume of research conducting such investigations at low temperatures particularly for catalysis applications, there is limited past work of the same type at high temperatures due to the challenges of the measurements at high temperature

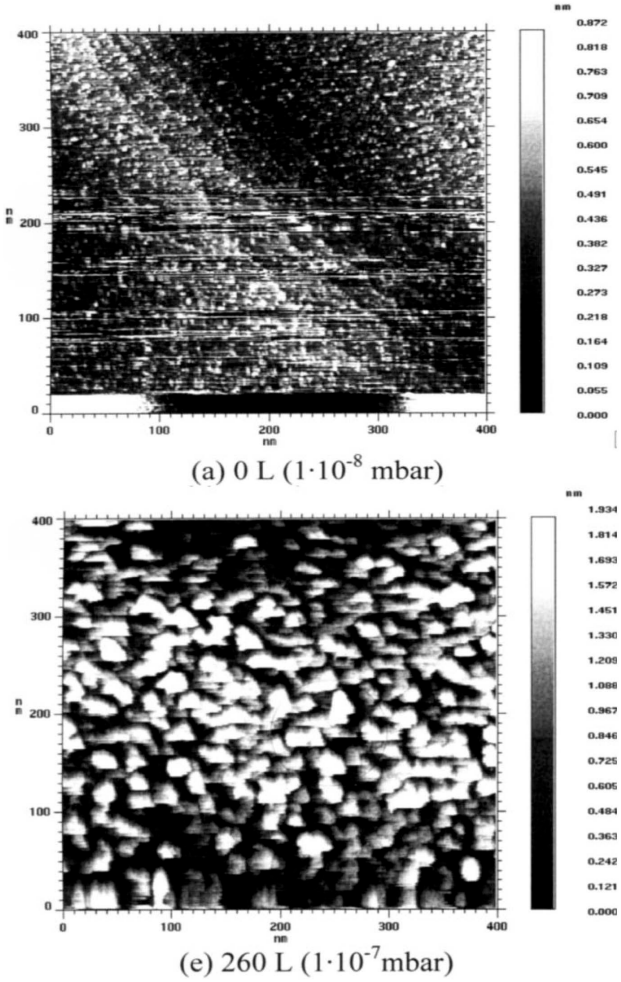


Fig. 11. Evolution of Surface Morphology by the Formation of $Cr_2O_3$ Clusters on Single Crystal Fe-15Cr during Oxidation at 440°C, Probed by Scanning Tunneling Microscopy. Figure Taken from [115]

and in the presence of fluids. A recent work worth mentioning here is that of Park and co-workers on Fe-Cr surfaces [115]. In this work, a single crystal of Fe-15Cr (100) was oxidized at 440°C under controlled oxygen partial pressure in a UHV system and the surface morphology was observed using *in situ* STM. The chemistry of the surface oxide layers was studied by XPS. Preparation of the single crystal in the UHV system did not lead to segregation of Cr to the surface during heating. *In situ* STM investigation at high temperature and controlled partial pressure of oxygen showed that oxidation of Fe-Cr commenced by nucleation of $Cr_2O_3$ on the surface (Fig.11) at 440°C, due to selective oxidation of Cr. When the Cr at the surface and at the interface was completely consumed by nucleation of Cr oxide, Fe oxidized and covered the initial Cr oxide nuclei, resulting in an Fe oxide layer on the surface. This work is a unique example for the capabilities that should be explored for fundamental investigations of surfaces and interfaces at chemo-mechanically active conditions. Such capabilities will be invaluable for the efforts of correlating transport processes in oxidation kinetics and passivity to the interface structure of nuclear structural metals.

## 5. OUTLOOK

Materials failure under high temperatures and stress, and in harsh chemical and radiation environments is a timely scientific challenge with far-reaching impact in major nuclear technology enterprises. It involves premature and catastrophic failure due to a complex combination of stresses and corrosive reactions further accelerated in the presence of high radiation fluxes. Atomistic-level understanding of corrosion initiation mechanisms is critical to microstructure optimization leading to the design of materials resistant to stress corrosion cracking. This is possible through the development of chemo-mechanical models capable of describing crack tip behavior in an environment of high temperature, chemical attack, and concentrated stress loading. Such models will have to be significantly more sophisticated than the crack propagation models currently available. In studying stress corrosion cracking, computational methods have the distinct advantage of allowing the application of exactly defined stress loads and chemical and radiation environments on fully characterized materials. Using atomistic simulations to demonstrate stress corrosion cracking, different size domains will have to be considered, with each requiring a different computational approach. The domains need to be nested, as regions far from process zones do not require the detailed description necessary for accurate prediction near the crack tip. These simulations, in combination with spectroscopic and microscopic *in situ* characterization of the early stages of corrosion, can be used to extract atomistic-level understanding of the basic mechanisms underlying stress corrosion cracking. Implementation of this strategy will require eventually large-scale simulations on petascale computing platforms. What we have sketched here is but a first step toward a long-term vision.

## ACKNOWLEDGEMENTS

B.Y acknowledges the discussions and collaboration with H. You for the *in situ* x-ray studies. S.Y and B.Y acknowledge discussions with R. G. Ballinger and A. Caro. S.Y acknowledges collaborations with J. Li and T. Zhu and discussions with N. Marzari, and P. Vashishta.

## REFERENCES

[ 1 ] Y. Guérin, G. S. Was, S. J. Zinkle, "Materials Challenges for Advanced Nuclear Energy Systems", *MRS Bulletin*, **34**, 1, pp. 10-19 (2009)

[ 2 ] D. Petti, D. Crawford, N. Chauvin, "Fuels for Advanced Nuclear Energy Systems", *MRS Bulletin*, **34**, 1, pp. 40-45 (2009)
[ 3 ] T. Allen, H. Burlet, R.K. Nanstad, M. Samaras, S. Ukai, "Advanced Structural Materials and Cladding", *MRS Bulletin*, **34**, 1, pp. 20-27 (2009)
[ 4 ] J-P. Bonal, A. Kohyama, Jaap van der Laan, L. Snead, "Graphite, Ceramics, and Ceramic Composites for High-Temperature Nuclear Power Systems", *MRS Bulletin*, **34**, 1, pp. 28-34 (2009)
[ 5 ] C. Cabet, J. Jang, J. Konys, P.F. Tortorelli, "Environmental Degradation of Materials in Advanced Reactors", *MRS Bulletin*, **34**, 1, pp. 35-39 (2009)
[ 6 ] W. Weber, A. Navrotsky, S. Stefanovsky, E. Vance, E. Vernaz, "Materials Science of High-Level Nuclear Waste Immobilization", *MRS Bulletin*, **34**, 1, pp. 46-53 (2009)
[ 7 ] M. F. Toney, A. J. Davenport, L. J. Oblonsky, M. Ryan, and C. M. Vitus, "Atomic Structure of the Passive Oxide Film Formed on Iron", *Phys. Rev. Lett*., **79**, 21, pp. 4282 - 4285 (1997)
[ 8 ] M. P. Ryan, R. C. Newman, and G. E. J. Thompson, "An STM Study of the Passive Film Formed on Iron in Borate Buffer Solution", *Electrochem. Soc*., **142**, 10, p. L177-L179 (1995)
[ 9 ] NSF Report, Simulation-Based Engineering Science, (2006)
[10] DOE-Basic Energy Sciences Workshop Report, Basic Research Needs for Advanced Nuclear Energy Systems, (2006)
[11] J. J. dePablo and W. A. Curtin, "Multiscale Modeling in Advanced Materials Research: Challenges, Novel Methods, and Emerging Applications", *MRS Bulletin*, **32**, 11, pp. 905-911 (2007)
[12] S. Yip, "Synergistic science", *Nature*, **2**, pp. 3-5 (2003)
[13] S. Yip, ed. Handbook of Material Modeling. Springer (2005)
[14] R. Najafabadi and S. Yip, "Observation of finite-temperature bain transformation (f.c.c. to r b.c.c.) in Monte Carlo simulation of iron", *Scripta Metall*, **17**, 10, pp. 1199-1204 (1983)
[15] K. S. Cheung, R. J. Harrison, S. Yip, "Stress induced martensitic transition in a molecular dynamics model of alpha-iron", *J. Appl. Phys*., **71**, 8, pp. 4009-4014 (1992)
[16] B. deCelis, A. S. Argon, S. Yip, "Molecular dynamics simulation of crack tip processes in alpha-iron and copper", *J. Appl. Phys*., **54**, 9, p. 4864 (1983)
[17] K. S. Cheung and S. Yip, "Brittle-ductile transition in intrinsic fracture behavior of crystals", *Phys. Rev. Lett*., **65**, 22, pp. 2804 - 2807 (1990)
[18] K. S. Cheung, A. S. Argon, S. Yip, "Activation analysis of dislocation nucleation from crack tip in alpha-Fe", *J. Appl. Phys*., **69**, 4, pp. 2088-2096 (1991)
[19] K. S. Cheung and S. Yip, "A molecular-dynamics simulation of crack-tip extension: The brittle-to-ductile transition", *Modell. Simul. Mater. Sci. Eng*., **2**, pp. 865-892 (1994)
[20] T. Kwok, P. S. Ho, S. Yip, "Molecular-dynamics studies of grain-boundary diffusion. I. Structural properties and mobility of point defects", *Phys. Rev. B*, **29**, 10, pp. 5354 - 5362 (1984a)
[21] T. Kwok, P. S. Ho, S. Yip, "Molecular-dynamics studies of grain-boundary diffusion. II. Vacancy migration, diffusion mechanism, and kinetics", *Phys. Rev. B*, **29**, 10, pp. 5363 - 5371 (1984b)
[22] C. J. Först, J. Slycke, K. J. Van Vliet, S. Yip, "Point Defect Concentrations in Metastable Fe-C Alloys", *Phys. Rev. Lett*., **96**, 175501, pp. 1-4 (2006)
[23] T. T. Lau, C. J. Foerst, J. D. Gale, S. Yip, K. J. Van Vliet, "Many-Body Potential for Point Defect Clusters in Fe-C Alloys", *Phys. Rev. Lett*., **98**, 215501, pp. 1-4 (2007)
[24] J. Li, "The Mechanics and Physics of Defect Nucleation", *MRS Bulletin*, **32**, pp. 151-159 (2007)
[25] M. Born, "On the stability of crystal lattices. I", *Cambridge Philos. Soc*., **36**, 2, pp. 160-172 (1940)
[26] M.Born and K. Huang. Dynamical theory of Crystal Lattices. Clarendon, Oxford (1956)
[27] R. Hill, "On the elasticity and stability of perfect crystals at finite strain", *Math. Proc. Camb. Phil. Soc*., **77**, 1, p. 225 (1975)
[28] R. Hill and F. Milstein, "Principles of stability analysis of ideal crystals", *Phys. Rev. B*, **15**, 6, pp. 3087 - 3096 (1977)
[29] J. Wang, J., Li, S. Yip, S. Phillpot, D. Wolf, "Mechanical instabilities of homogeneous crystals", *Phys. Rev. B*, **52**, 17, pp. 12627 - 12635 (1995)
[30] Z. Zhou and B. Joos, "Stability criteria for homogeneously stressed materials and the calculation of elastic constants", *Phys. Rev. B*, **54**, 6, pp. 3841 - 3850 (1996)
[31] J. W. Morris and C. R. Krenn, "The internal stability of an elastic solid", *Philos Mag. A*, **80**, 12, pp. 2827-2840 (2000)
[32] D. Roundy, C. R. Krenn, L. Cohen Marvin, J. W. Morris Jr., "Ideal Shear Strengths of fcc Aluminum and Copper", *Phys. Rev. Lett*., **82**, 13, pp. 2713-2716 (1999)
[33] S. Ogata , J. Li, S. Yip, "Ideal Pure Shear Strength of Aluminum and Copper", *Science*, **298**, pp. 807-811 (2002)
[34] T. H. K. Barron and M. L. Klein, "Second-order elastic constants of a solid under stress", *Proc. Phys. Soc*., **85**, pp. 523-532 (1965)
[35] W. G. Hoover, A. C. Holt, D. R. Squire, "Adiabatic elastic constants for argon. theory and Monte Carlo calculations", *Physica*, **44**, 3, pp. 437-443 (1969)
[36] Z. S. Basinski, M. S. Duesbery, A. P. Pogany, R. Taylor, Y. P. Varshni, "An effective ion-ion potential for sodium", *Can. J. Phys*., **48**, pp. 1480-1489 (1970)
[37] J. Wang, S. Yip, S. Phillpot, D. Wolf, "Crystal instabilities at finite strain", *Phys. Rev. Lett*., **71**, 25, pp. 4182 - 4185 (1993)
[38] K. Mizushima, S. Yip, E. Kaxiras, "Ideal crystal stability and pressure-induced phase transition in silicon", *Phys. Rev. B*, **50**, 20, pp. 14952 - 14959 (1994)
[39] M. Tang and S. Yip, "Lattice instability in -SiC and simulation of brittle fracture", *J. Appl. Phys*., **76**, 5, pp. 2719-2725 (1994)
[40] F. Cleri, J. Wang, S. Yip, "Lattice instability analysis of a prototype intermetallic system under stress", *J. Appl. Phys*., **77**, 4, p. 1449 (1995)
[41] M. Tang and S. Yip, "Atomic Size Effects in Pressure-Induced Amorphization of a Binary Covalent Lattice", *Phys. Rev. Lett*., **75**, 14, pp. 2738 - 2741 (1995)
[42] J. Li and S. Yip, "Atomistic Measures of Materials Strength", *Computer Modelling in Engineering and Sciences*, **3**, 2, pp. 219-227 (2002)
[43] J. Tersoff, "Modeling solid-state chemistry: Interatomic potentials for multicomponent systems", *Phys. Rev. B*, **39**, 8, pp. 5566 - 5568 (1989)
[44] J. Li, Ph.D. Thesis, MIT, (2000)
[45] F. Cleri, S. Yip, D. Wolf, S. Phillpot, "Atomic-Scale

Mechanism of Crack-Tip Plasticity: Dislocation Nucleation and Crack-Tip Shielding", *Phys. Rev. Lett.*, **79**, 7, pp. 1309 - 1312 (1997)
[46] H. Jonsson, G. Mills, K. W. Jacobsen. Classical and Quantum Dynamics in Condensed Phase Simulations. Plenum Press, New York, p.385 (1998)
[47] T. Zhu, J. Li, S. Yip, "Atomistic Study of Dislocation Loop Emission from a Crack Tip", *Phys. Rev. Lett.*, **93**, 025503, pp. 1-4 (2004)
[48] T. Zhu, J. Li, S. Yip, "Atomistic Configurations and Energetics of Crack Extension in Silicon", *Phys. Rev. Lett.*, **93**, 205504, pp. 1-4 (2004)
[49] Y. Mishin, M. J. Mehl, D. A. Papaconstantopoulos, A. F. Voter and J. D. Kress, "Structural stability and lattice defects in copper: Ab initio, tight-binding, and embedded-atom calculations", *Phys. Rev. B*, **63**, 224106, pp. 1-16 (2001)
[50] F. H. Stillinger and T. A. Weber, "Computer simulation of local order in condensed phases of silicon", *Phys. Rev. B*, **31**, 8, pp. 5262-5271 (1985)
[51] J. R. Rice, "Dislocation nucleation from a crack tip: An analysis based on the Peierls concept", *J. Mech. Phys. Solids*, **40**, 2, pp. 239-271 (1992)
[52] G. Xu, A. S. Argon, M. Ortiz, "Critical configurations for dislocation nucleation from crack tips", *Philos. Mag. A*, **75**, 2, pp. 341-367 (1997)
[53] A. N. Stroh, "Dislocations and cracks in anisotropic elasticity," *Philos. Mag.*, **7**, p. 625 (1958)
[54] H.-L. Sit, M. Cococcioni, and N. Marzari, "Realistic Quantitative Descriptions of Electron Transfer Reactions: Diabatic Free-Energy Surfaces from First-Principles Molecular Dynamics", *Phys. Rev. Lett.*, **97**, 028303, pp. 1-4 (2006)
[55] H. J. Kulik, M. Cococcioni, D. A. Scherlis, and N. Marzari, "Density Functional Theory in Transition-Metal Chemistry: A Self-Consistent Hubbard U Approach", *Phys. Rev. Lett.*, **97**, 103001, pp. 1-4 (2006)
[56] D. A. Scherlis, J.-L. Fattebert, F. Gygi, M. Cococcioni, and N. Marzari, "A unified electrostatic and cavitation model for first-principles molecular dynamics in solution", *J. Chem. Phys.*, **124**, 074103, pp. 1-12 (2006)
[57] S. C. Hendy, N. J. Laycock, M. P. Ryan, and B. E. Walker, "Ab initio studies of the passive film formed on iron", *Phys. Rev. B*, **67**, 085407, pp. 1-10 (2003)
[58] S. C. Hendy, N. J. Laycock, and M. P. Ryan, "Atomistic Modeling of Cation Transport in the Passive Film on Iron and Implications for Models of Growth Kinetics", *J. Electrochem. Soc.*, **152**, 8, p. B271-B276 (2005)
[59] N. Cabrera and N. F. Mott, "Theory of the oxidation of metals", *Rep. Prog. Phys.*, **12**, pp. 163-184 (1948/1949)
[60] V. S. Battaglia and J. Newman, "Modeling of a Growing Oxide Film: The Iron/Iron Oxide System", *J. Electrochem. Soc.*, **142**, 5, pp. 1423-1430 (1995)
[61] D. D. MacDonald, "Passivity - the key to our metals-based civilization", *Pure and Applied Chemistry*, **71**, 6, p. 951 (1999)
[62] C. G. Van de Walle and J. Neugebauer, "Universal alignment of hydrogen levels in semiconductors, insulators and solutions", *Nature*, **423**, pp. 626 - 628 (2003)
[63] QuantumEspresso. http://www.quantum-espresso.org/
[64] Y. Tanaka et al., "A study on the Fermi surface of Cr by high-resolution Compton scattering", *Journal of Physics and Chemistry of Solids*, **61**, 3, pp. 365-367 (2000)
[65] V. Maurice, G. Despert, S. Zanna, M. P. Bacos, and P. Marcus, "Self-assembling of atomic vacancies at an oxide/intermetallic alloy interface", *Nature Materials*, **3**, pp. 687-691 (2004)
[66] G. S. Frankel, "Pitting Corrosion of Metals", *J. Electrochem. Soc.*, **145**, 6, pp. 2186-2198 (1998)
[67] M. P. Ryan, D. E. Williams, R. J. Chater, B. M. Hutton, and D. S. McPhail, "Why stainless steel corrodes", *Nature*, **415**, 2, pp. 770 - 774 (2002)
[68] C. Punckt, M. Bölscher, H. H. Rotermund, A. S. Mikhailov, L. Organ, N. Budiansky, J. R. Scully, and J. L. Hudson, "Sudden Onset of Pitting Corrosion on Stainless Steel as a Critical Phenomenon", *Science*, **305**, pp. 1133-1136 (2004)
[69] F. Shimizu, S. Ogata and J. Li, "Yield point of metallic glass", *Acta Mater.*, **54**, 16, pp. 4293-4298 (2006)
[70] T. Zhu, J. Li, K. J. Van Vliet, S. Ogata, S. Yip, S. Suresh, "Predictive modeling of nanoindentation-induced homogeneous dislocation nucleation in copper", *J. Mech. Phys Solids*, **52**, 3, pp. 691-724 (2004)
[71] T. Zhu, J. Li, A. Samanta, H. G. Kim, S. Suresh, "Interfacial plasticity governs strain rate sensitivity and ductility in nanostructured metals", *Proc. Nat. Acad. Sci*, **104**, 9, pp. 3031-3036 (2007)
[72] D. E. Williams, R. C. Newman, Q. Song, R. G. Kelly, "Passivity breakdown and pitting corrosion of binary alloys", *Nature*, **350**, 1, pp. 216 - 219 (1991)
[73] S. N. Rashkeev, K.W. Sohlberg, S. Zhuo, S. T. Pantelides, "Hydrogen-Induced Initiation of Corrosion in Aluminum", *J. Phys. Chem. C*, **111**, 19, pp. 7175-7178 (2007)
[74] S. M. Bruemmer, G.S. Was, "Microstructural and microchemical mechanisms controlling intergranular stress corrosion cracking in light-water-reactor systems", *Journal of Nuclear Materials*, **216**, pp. 348-363 (1994)
[75] G.S. Was, B.Alexandreanu, P. Andresen, and M. Kumar, Mat. Res. Soc. Symp. Proc. 819, N2.1.1 (2004, "Role of Coincident Site Lattice Boundaries in Creep and Stress Corrosion Cracking", *Mat. Res. Soc. Symp. Proc.*, **819**, p. N2.1.1 (2004)
[76] S.M. Bruemmer, "Linking Grain Boundary Structure and Composition to Intergranular Stress Corrosion Cracking of Austenitic Stainless Steels", *MRS Symposium Proceedings*, **819**, 2.2.1, pp. 1-10 (2004)
[77] S. Teysseyre, and G.S. Was, "Stress Corrosion Cracking of Austenitic Alloys in Supercritical Water", *Corrosion*, **62**, 12, pp. 1100-1116 (2006)
[78] B. Alexandreanu, B.H. Sencer, V. Thaveeprunsriporn, G.S. Was, "The effect of grain boundary character distribution on the high temperature deformation behavior of Ni-16Cr-9Fe alloys", *Acta Materialia*, **51**, 13, pp. 3831-3848 (2003)
[79] D.N. Seidman, "Subnanoscale studies of segregation at grain boundaries: Simulations and Experiments", *Annu. Rev. Mater. Sci.*, **32**, pp. 235-269 (2002)
[80] D. Wolf. in Handbook of Material Modeling, sec. 6.9 Springer (2005)
[81] A. P. Sutton and R. W. Balluffi. Interfaces in Crystalline Materials. Oxford University Press, Oxford (1995)
[82] M. Ropo, K. Kokko, M. P. J. Punkkinen, S. Hogmark, J. Kollár, B. Johansson, L. Vitos, "Theoretical evidence of the compositional threshold behavior of FeCr surfaces", *Phys. Rev. B*, **76**, 220401, pp. 1-4 (2007)
[83] L. Vitos, I. A. Abrikosov, and B. Johansson, "Anisotropic Lattice Distortions in Random Alloys from First-Principles

Theory", *Phys. Rev. Lett.*, **87**, 156401, pp. 1-4 (2001)
[84] P. Hohenberg, W. Kohn, "Inhomogeneous Electron Gas", *Physical Review*, **136**, 3B, pp. 864-871 (1964)
[85] J. P. Perdew, K. Burke, M. Ernzerhof, "Generalized Gradient Approximation Made Simple", *Phys. Rev. Lett.*, **77**, 18, pp. 3865 - 3868 (1996)
[86] L. Dubrovinsky et al., "Iron-silica interaction at extreme conditions and the electrically conducting layer at the base of Earth's mantle", *Nature* (*London*), **422**, pp. 58-61 (2003)
[87] M. Aldén, H. L. Skriver, S. Mirbt, B. Johansson, "Surface energy and magnetism of the 3d metals", *Surface Science*, **315**, 1-2, pp. 157-172 (1994)
[88] N. Kumar Das, K. Suzuki, Y. Takeda, K. Ogawa, T. Shoji, "Quantum chemical molecular dynamics study of stress corrosion cracking behavior for fcc Fe and Fe-Cr surfaces", *Corrosion Science*, **50**, 6, pp. 1701-1706 (2008)
[89] A. Ramasubramaniam, E. Carter, "Coupled Quantum-Atomistic and Quantum-Continuum Mechanics Methods in Materials Research", *MRS Bulletin*, **32**, pp. 913-918 (2007)
[90] A.C.T. van Duin, S. Dasgupta, F. Lorant, W.A. Goddard, "ReaxFF: A Reactive Force Field for Hydrocarbons", *J. Phys. Chem. A*, **105**, 41, p. 9396-9409 (2001)
[91] A.C.T. van Duin, A. Strachan, S. Stewman, Q. Zhang, X. Xu, W.A. Goddard, "ReaxFFSiO Reactive Force Field for Silicon and Silicon Oxide Systems", *J. Phys. Chem A*, **107**, 19, pp. 3803-3811 (2003)
[92] M. J. Buehler, A. C. T. van Duin,W. A. Goddard, "Multiparadigm Modeling of Dynamical Crack Propagation in Silicon Using a Reactive Force Field", *Phy. Rev. Lett.*, **96**, 095505, pp. 1-4 (2006)
[93] A. Caro, D. A. Crowson, M. Caro, "Classical Many-Body Potential for Concentrated Alloys and the Inversion of Order in Iron-Chromium Alloys", *Phys. Rev. Lett.*, **95**, 075702, pp. 1-4 (2005)
[94] P. Erhart, B. Sadigh, A. Caro, "Are there stable long-range ordered Fe1-xCrx compounds?", *Appl. Phys. Lett.*, **92**, 141904, pp. 1-3 (2008)
[95] L. Malerba, A. Caro, J. Wallenius, "Multiscale modelling of radiation damage and phase transformations: The challenge of FeCr alloys", *J. Nuc. Matls*, accepted, (2008)
[96] A. Yilmazbayhan, E. Breval, A. T. Motta, R.J. Comstock, "Transmission electron microscopy examination of oxide layers formed on Zr alloys", *J. Nuc. Matls*, **349**, 3, pp. 265-281 (2006)
[97] Y. Fujii, E. Yanase, K. Arai, "Depth profiling of the strain distribution in the surface layer using X-ray diffraction at small glancing angle of incidence", *Appl. Surf. Sci.*, **244**, 1-4, p. 230 (2005)
[98] A. Yilmazbayhan, A. T. Motta, R J. Comstock, G. P. Sabol, B. Lai, Z. Cai, "Structure of zirconium alloy oxides formed in pure water studied with synchrotron radiation and optical microscopy: relation to corrosion rate", *J. Nuc. Matls.*, **324**, 1, pp. 6-22 (2004)
[99] M. Yamashita, H. Konishi, J. Mizuki, et al., "Nanostructure of Protective Rust Layer on Weathering Steel Examined Using Synchrotron Radiation X-rays", *Materials Trans.*, **45**, 6, pp. 1920-1924 (2004)
[100] M. Yamashita, H. Konishi, T. Kozakura, et al., "In situ observation of initial rust formation process on carbon steel under Na2SO4 and NaCl solution films with wet/dry cycles using synchrotron radiation X-rays", *Corrosion Science*, **47**, 10, pp. 2492-2498 (2005)
[101] S.K. Sinha, E.B. Sirota, S. Garoff, H.B. Stanley, "X-ray and neutron scattering from rough surfaces", *Phys. Rev. B*, **38**, 4, pp. 2297 - 2311 (1988)
[102] H. You, C.A. Melendres, Z. Nagy, V.A. Maroni, W. Yun, R.M. Yonco, "X-ray-reflectivity study of the copper-water interface in a transmission geometry under in situ electrochemical control", *Phys. Rev. B*, **45**, 19, pp. 11288 - 11298 (1992)
[103] Y.P. Feng, S.K. Sinha, C.A. Melendres, D.D. Lee, "X-ray off-specular reflectivity studies of electrochemical pitting of Cu surfaces in sodium bicarbonate solution", *Physica B 221 p. 251* (*1996*, **221**, 1-4, pp. 251-256 (1996)
[104] H. You, Z. Nagy, and K. Huang, "X-Ray Scattering Study of Porous Silicon Growth during Anodic Dissolution", *Phys. Rev. Lett.*, **78**, 7, pp. 1367 - 1370 (1997)
[105] P.F. Fewster, N.L. Andrew, V. Holy, K. Barmak, "X-ray diffraction from polycrystalline multilayers in grazing-incidence geometry: Measurement of crystallite size depth distribution", *Phys. Rev. B*, **72**, 174105, pp. 1-11 (2005)
[106] S. Sembiring, B. O'Connor, D. Li, A. van Riessen, C. Buckley, I. Low, R. De Marco, "Advances in X-ray Analysis", *Proceedings of the Denver X-ray Conference*, **43**, (1999)
[107] D. H. Kim, H. H. Lee, S. S. Kim, H. C. Kang, D. Y. Noh, H. Kim, S. K. Sinha, "Chemical depth profile of passive oxide on stainless steel", *Appl. Phys. Lett.*, **85**, 26, pp. 6427-6429 (2004)
[108] J.J. Rehr, R.C. Albers, "Theoretical approaches to x-ray absorption fine structure", *Rev. Mod. Phys.*, **72**, 3, pp. 621 - 654 (2000)
[109] B. Yildiz, K.-C. C. Chang, H. You, D. Miller, H. Bearat, and M. McKelvy, *212th Meeting of the Electrochemical Society*, Washington, DC (2007)
[110] J. Diefenbacher, M. McKelvy, A.V.G. Chizmeshya, G.H. Wolf, "Externally controlled pressure and temperature microreactor for in situ x-ray diffraction, visual and spectroscopic reaction investigations under supercritical and subcritical conditions", *Rev. Sci. Inst.*, **76**, 1, pp. 015103-015101 (2005)
[111] C.T. Fujii, R.A. Meussner, "The Mechanism of the High-Temperature Oxidation of Iron-Chromium Alloys in Water Vapor", *J. Electrochem. Soc.*, **111**, pp. 1215-1221 (1964)
[112] L.B. Kriksunov, D.D. Macdonald, "Corrosion in Supercritical Water Oxidation Systems: A Phenomenological Analysis", *J. Electrochem. Soc.*, **142**, p. 4069 (1995)
[113] C.-M. Liao, J.M. Olive, M. Gao, R.P. Wei, "In-Situ Monitoring of Pitting Corrosion in Aluminum Alloy 2024", *Corrosion*, **54**, 6, p. 451-458 (1998)
[114] F. A. Martin, C. Bataillon, J. Cousty, "In situ AFM detection of pit onset location on a 304L stainless steel", *Corrosion Science*, **50**, 1, pp. 84-92 (2008)
[115] E. Park, B. Huning, S. Borodin, M. Rohwerder, and M. Spiegel, "Initial oxidation of Fe-Cr alloys: in situ STM and ex situ SEM observation", *Materials at High Temperatures*, **22**, 3/4, pp. 567-573 (2005)
[116] T. Zhu, J. Li, S. Yip, "Nanomechanics of Crack Front Mobility", *J. Appl. Mech.*, **72**, 6, pp. 932-935 (2005)